Road Roughness Level Identification Based on BiGRU Network

SHUANG CHEN AND JUNJUN XUE

College of Automotive and Traffic Engineering, Liaoning University of Technology, Jinzhou 121001, China

Corresponding author: Shuang Chen (cslxy74@163.com)

ABSTRACT A new method of road roughness level identification based on the bidirectional gated recurrent unit (BiGRU) network is proposed in this paper, which is contribute to solve the problems of intelligent chassis technology such as suspension control. Firstly, the vehicle vibration response data is attained by the ride comfort simulation of two-degree-of-freedom vehicle vibration model. Then the mapping relationship between the road roughness level and the vehicle vibration responses is determined, and the road roughness level identification model is established. The Adam algorithm and mini-batch gradient descent are utilized to improve the accuracy and increase the speed of the model training process. Finally, in order to verify the feasibility and practicability of the model, the ride comfort experiments are carried out on asphalt and brick roads. The results show that the accuracy of the road roughness level identification model based on the BiGRU network reaches 95.83%, and the recognition result is reliable. Moreover, the experimental road level can be successfully identified through the road roughness level identification model, which has high engineering application value.

INDEX TERMS GRU, road roughness level identification, reverse analysis, vehicle responses.

I. INTRODUCTION

To car in the process of driving, the road uneven is the most important excitation source for vehicle vibration. Accurate road excitation information is of great significance to vehicle dynamics control, especially suspension control. It is impossible to use the same set of suspension control parameters to meet synchronously the requirements of ride comfort and driving safety. Therefore, road roughness level information can provide a direct basis for parameter adjustment in suspension control. At present, the common methods for obtaining road information include the measurement and the reverse analysis.

Measurement methods include direct measurement and non-contact measurement. To the direct measurement method, the road roughness measuring instrument is used to directly measure the road roughness [1]. However, the direct measurement method cannot achieve real-time on-board measurement, so it is rarely applied at present. To the Non-contact measurement method, the laser radar, infrared, vehicle cameras and other equipment are used to extract road

information. Ž. Vidas *et al.* [2] used image analysis and laser scanning to identify road types. M. A. Bekhti *et al.* [3] extracted the road features by collecting images of the road ahead, and established the relationship between the road and the vibration of the vehicle, predicted the vibration of the vehicle. Q. Liu *et al.* [4] established a road recognition model based on convolution neural networks, which can accurately identify a variety of roads. S. Wang *et al.* [5] used image feature data fusion methods to identify non-urban roads, and BP neural Network is used for classification. H. Xu [6] used millimeter-wave radar to study the radar scattering area and time-frequency map to identify the road. Although the non-contact measurement method obtains a wide range of roads, it is costly and sensitive to weather and other conditions.

In the reverse analysis method, the acceleration sensors and displacement sensors are installed on relevant position of vehicle, and the reverse identification of the roads are completed by obtaining the vehicle vibration response of different roads. H. M. Ngwangwa *et al.* [7], [8] collected vehicle vibration response information and used neural network methods to identify Belgian roads. T. H. Nguyen *et al.* [9] detected the state of the road surfaces based on vehicle response and

random forest methods, and then perform roads classification and identification. C. Lin *et al.* [10] established the road roughness prediction model based on NARX neural network and used vehicle responses to predict road roughness. J. Li *et al.* [11], [12] predicted road roughness based on the reverse analysis of vehicle vibration response. By comparing four typical neural networks, namely BP neural network, RBF neural network, wavelet neural network and NARX neural network, it shows that NARX neural network has the best effect in predicting road roughness. Y. Wang *et al.* [13] used the intelligent tire road recognition algorithm based on support vector machine to study the road level recognition. Although the real-time performance is not as good as that of the measurement method, it is not easily affected by factors such as weather, light, dust, etc., and the cost is low.

With the gradual popularization of artificial intelligence, deep learning algorithm has being a research hotspot in recent years. Its advantage lies in the non-linear mapping of the data feature layer and the ability to automatically construct deep features. In addition, there is no need to manually select feature parameters, and it has good generalization ability. At present, deep learning algorithm has made certain developments in the field of intelligent transportation systems and vehicles, such as traffic flow prediction [14], environment perception [15], [16] and driving behavior recognition [17]. L. Cheng *et al.* [18] proposed a convolution neural network model with an improved activation function to classify road conditions. G. Liang *et al.* [19] identified the road roughness level in real time based on the LSTM network and time-series wheel center acceleration. The results show that the algorithm has high accuracy in identifying road roughness. Inspired by deep learning, the reverse analysis of vehicle vibration responses based on BiGRU network is proposed to identify the road roughness level in this paper. Firstly, the road roughness level identification model is designed. Secondly, by the two-degree-of-freedom vehicle vibration model ride comfort simulation experiment, the vehicle vibration response signals of different levels of roads are obtained. Then, the vehicle vibration response data set is used to train and test the road roughness level identification model. Finally, in order to verify the feasibility and practicability of the model, the ride comfort experiments are carried out on typical roads, and the road roughness level identification model is used to identify the experimental road.

II. ROAD ROUGHNESS LEVEL IDENTIFICATION MODEL
In this paper vehicle vibration responses will be used to reversely recognize the road level, so the road roughness level identification model based on the BiGRU network is established. The recognition process is shown in Fig. 1.

A. THE STRUCTURE OF THE ROAD ROUGHNESS LEVEL IDENTIFICATION MODEL
The road roughness level identification model is mainly composed of an input layer, a BiGRU layer, a fully connected layer, and an output layer. The structure of the identification
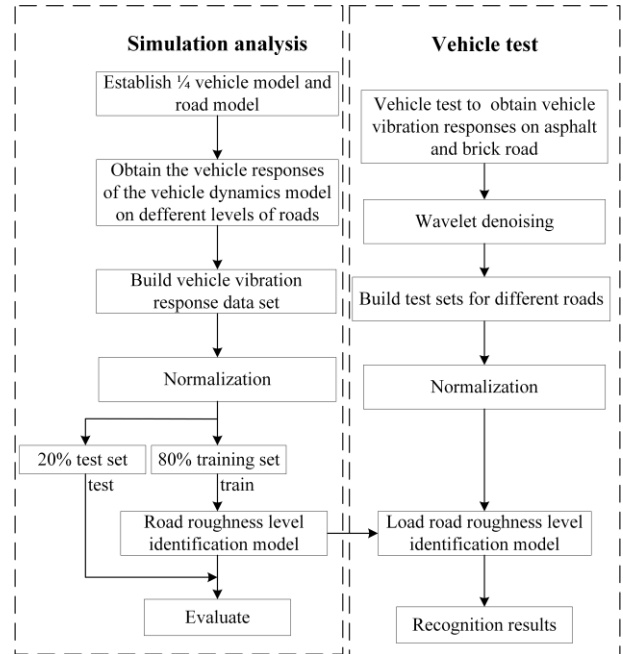

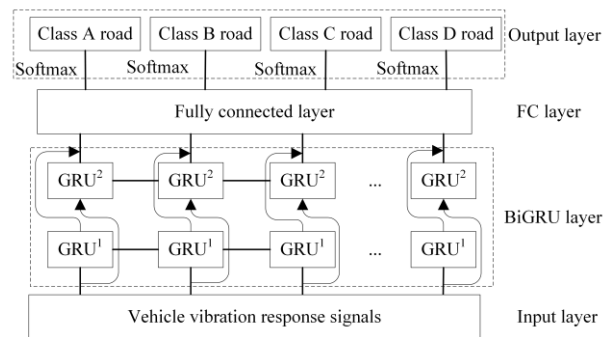FIGURE 1. Process of road roughness level identification.

FIGURE 2. The structure of the road roughness level identification model.

mode is shown in Fig. 2. Firstly, as the input of the model the vehicle vibration response data are processed by the BiGRU network to extract the time series structural features. Then, the output vector of the BiGRU network is used as the input of the fully connected layer for classification. Finally, the Softmax function is used in the output layer to output the road roughness levels include the class A road, the class B road, the class C road, and the class D road.

B. INPUT LAYER
The input of the road roughness level identification model is:

$$X_t = \{\alpha_1(t), \alpha_2(t)\} \tag{1}$$

where X_t represents the model input vector at the moment of t; $\alpha_1(t)$ is the body acceleration; $\alpha_2(t)$ is the wheel acceleration. Each group of sample data is determined as 100 moments according to the size of the sliding window.
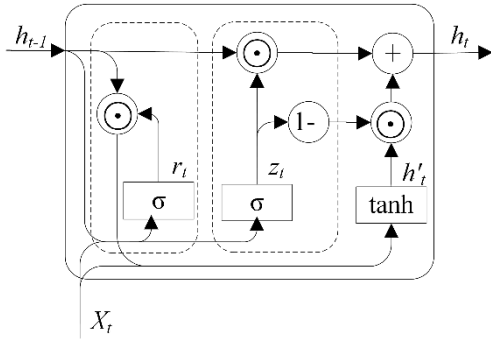
FIGURE 3. GRU unit.

C. BIGRU LAYER

Long short-term memory network (LSTM) [20] is used to adjust the flow of information by introducing a gating mechanism to remember long-term timing information, and solves the problems of gradient disappearance and gradient explosion in traditional recurrent neural networks. However, the LSTM network model has a complex structure and a long training time. In 2014, K. Cho *et al.* [21] proposed GRU to optimize the structure of LSTM, and its structure is shown in Fig. 3. GRU is a variant of LSTM network. It retains all the advantages of LSTM. The performance of the two kind of network is equal, but the structure of GRU network is simpler. It replaces the input gate and forget gate of LSTM with an update gate, and retains the original reset gate. In addition, the input of the activation function is adjusted by the weight parameter to retain useful information and discard irrelevant information, which makes GRU network capable of a strong memory [22]. GRU is unmatched by other neural networks in dealing with issues that are highly related to timing. The GRU network update weight parameter formula is as follows:

1) CALCULATION OF UPDATE GATE

The function of the update gate is to determine the amount of historical moment information added to the current moment, which is conduced to the capture of long-term dependencies in time series data. The amount of information retained at the previous moment is proportional to the value of the update gate.

$$z_t = \sigma(w_{xz}X_t + w_{hz}h_{t-1} + b_z) \tag{2}$$

where z_t is the update gate of the GRU network; X_t is the input vector of the GRU network at the moment of t; h_{t-1} is the output of the GRU network at the moment of $t-1$; w_{xz} and w_{hz} are the weight matrix of the update gate; b_z is the deviation parameter of the update gate; σ is the sigmoid function.

2) CALCULATION OF RESET GATE

The function of reset gate is to forget irrelevant information at the previous moment, which is conducive to the capture of short-term dependencies in time series data. The amount
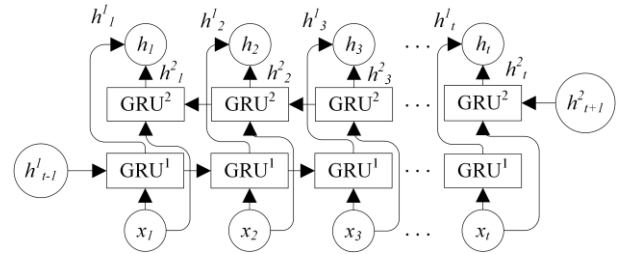

FIGURE 4. The structure of the BiGRU network.

of information ignored at the previous moment is inversely proportional to the value of the reset gate.

$$r_t = \sigma(w_{xr}X_t + w_{hr}h_{t-1} + b_r) \tag{3}$$

where r_t is the reset gate of the GRU network; w_{xr} and w_{hr} are the weight matrix of the reset gate; b_r is the deviation parameter of the reset gate.

3) RESET CURRENT MEMORY CONTENT

The reset gate is used to reset the memory information, and the activation function *tanh* is used to limit the current memory content to $[-1,1]$.

$$h'_t = tanh(w_{xh}X_t + r_t * w_{hh}h_{t-1} + b_h) \tag{4}$$

where h'_t is the memory content of the GRU network; w_{xh} and w_{hh} are the weight matrix; b_h is the deviation parameter; $*$ is the element-wise multiplication.

4) CALCULATE THE OUTPUT OF GRU NETWORK

The output of GRU network is composed of the output information at the previous moment and the current moment, and the update gate is used to control the inflow of the two types of information.

$$h_t = z_t * h_{t-1} + (1 - z_t) * h'_t \tag{5}$$

where h_t is the output of GRU network at the moment of t.

The traditional GRU network transmits information along single direction of the time series, and can only obtain historical moment information, ignore future moment information. Therefore, the BiGRU bidirectional network is adopted. The number of GRU network units is 200, which fully considers the historical and future moment information of the vehicle vibration response data. The structure of the BiGRU network is shown in Fig. 4. Here, GRU[1] represents a forward GRU, and GRU[2] represents a reverse GRU. The hidden layer state h_t of BiGRU at the moment of t is jointly determined by the forward hidden layer output h_t^1 and the reverse hidden layer output h_t^2.

D. FULLY CONNECER LAYER

The fully connected neural network does not require the dimensions of the input data, and has high reliability and low latency. It is the simplest and most basic neural network. Therefore, the fully connected neural network is used to
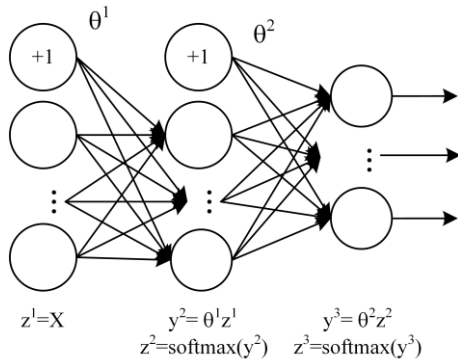
FIGURE 5. The structure of the fully connected neural network.

synthesize the feature information extracted by the BiGRU network to classify the road roughness level. The structure of the fully connected neural network is shown in Fig. 5. The output of the BiGRU network is used as the input of the fully connected neural network, and the number of output neurons is the same as the number of road level categories.

E. OUTPUT LAYER

In order to generate the recognition rate of each level of road, the Softmax function is selected in the output layer. The Softmax function can be continuously and differentiable, which ensure that the neural network always maintains a continuous state of convergence, avoid the occurrence of local optimal problems. It is suitable for dealing with multi-classification problems. The output vector of the fully connected layer is inputted into the Softmax function and mapped to the range of (0,1) to generate the probability of the road level categories, namely, class A road, class B road, class C road, and class D road. The output result is a 4-dimensional column vector. The Softmax function is shown in (6).

$$z^i = \mathrm{softmax}(y^i) = \frac{e^{y^i}}{\sum_K e^{y^i}} \tag{6}$$

where y^i is the output vector of the fully connected layer, and z^i is the recognition rate.

III. ACQUISITION OF VEHICLE VIBRATION RESPONSES
Deep learning requires a large amount of data for network training, and it is difficult to obtain a large amount of complete data for vehicle measurement. Therefore, the filtered white noise is used to generate different road roughness signals, and the network is trained by the vertical acceleration responses of the body and wheels obtained from the simulation of the suspension model.

A. RANDOM INPUT ROAD MODEL
Generally, the height change of road surface relative to reference plane and road direction are defined as the road roughness function [23]. The road roughness function is a random function. It is often considered that its mean value is zero and
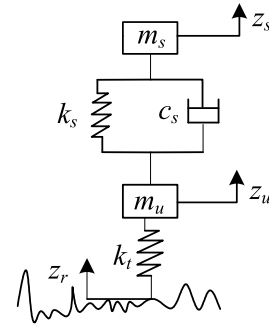
obeys a normal distribution. In addition, the power spectrum density is usually used to express its characteristics. The expression is:

$$G_q(n) = G_q(n_0) \left(\frac{n}{n_0} \right)^{-w} \tag{7}$$

where n is the spatial frequency(m^{-1}); w is the frequency index, usually $w = 2$; n_0 is the reference spatial frequency, the value is $0.1\mathrm{m}^{-1}$; $G_q(n_0)$ is the road roughness coefficient shown in Table 1 [24].

In this paper, the filtered white noise method is used to generate the road model in the time domain. The equation of road surface input is as follow:

$$\dot{z}_r(t) = -2\pi f_0 z_r(t) + 2\pi \sqrt{G_0} v w(t) \tag{8}$$

where f_0 is low cut-off frequency, the value is approximately 0.01 Hz; G_0 is the road roughness coefficient; $w(t)$ is a filtered white noise.

B. TWO-DEGREE-OF-FREEDOM VEHICLE VIBRATION MODEL
The two-degree-of-freedom vehicle vibration model has a simple structure and is widely used in the vertical dynamics of the suspension. The structure of the model is shown in Fig. 6:

FIGURE 6. The two-degree-of-freedom vehicle vibration model.

Here, $m_s, m_u, k_s, c_s, k_t, z_s, z_u, z_r$ are the body mass, wheel mass, suspension stiffness, suspension damping, tire stiffness, body vertical displacement, wheel vertical displacement, and road input displacement.

According to Newton's second law of motion, the dynamic differential equation is as follow:

$$m_s \ddot{z}_s + c_s (\dot{z}_s - \dot{z}_u) + k_s(z_s - z_u) = 0 \tag{9}$$
$$m_u \ddot{z}_u - c_s (\dot{z}_s - \dot{z}_u) - k_s(z_s - z_u) + k_t (z_u - z_r) = 0 \tag{10}$$

The state vector, output vector and state space equation are as follows:

$$X = [z_s - z_u, \dot{z}_s, z_u - z_r, \dot{z}_u]^T \tag{11}$$
$$Y = [\ddot{z}_s, z_s - z_u, z_u - z_r]^T \tag{12}$$
$$\begin{cases} \dot{X}(t) = AX(t) + Bw(t) \\ Y(t) = CX(t) \end{cases} \tag{13}$$

TABLE 1. Classification of Different Types of Roads.

Road roughness level	Road type
Class A road	Paved roads, including high-speed expressways, etc., roads are flat and less curved.
Class B road	Paved road, winding mountain road, flat, with a little gravel.
Class C road	Dirt road, gravel, continuous winding mountain road, slope 10°, and grade 2 road covered with snow and ice.
Class D road	More 10cm bumps, stones, 10cm deep long-distance dirt roads, unpaved roads with a slope of less than 18°, soft sandy ground and grade 3 road covered with ice and snow.

TABLE 2. Road Roughness Classification Standard.

Road roughness level	$G_q(n_0)/(10^{-6}m^3)(n_0=0.1m^{-1})$ Geometric mean
Class A road	16
Class B road	64
Class C road	256
Class D road	1024

TABLE 3. Vehicle Model Parameters.

Vehicle parameters	Unit	Value
Body mass	kg	305
Suspension stiffness	N/m	21000
Suspension damping	N/(m/s)	2000
Wheel mass	kg	45
Tire stiffness	N/m	200000

where $w(t)$ is white noise signal input, and the individual parameter matrices are as follows:

$$A = \begin{bmatrix} 0 & 1 & 0 & -1 \\ -\dfrac{k_s}{m_s} & -\dfrac{c_s}{m_s} & 0 & \dfrac{c_s}{m_s} \\ 0 & 0 & 0 & 1 \\ \dfrac{k_s}{m_u} & \dfrac{c_s}{m_u} & -\dfrac{k_t}{m_u} & -\dfrac{c_s}{m_u} \end{bmatrix} ; \quad B = \begin{bmatrix} 0 \\ 0 \\ -1 \\ 0 \end{bmatrix} ;$$

$$C = \begin{bmatrix} -\dfrac{k_s}{m_s} & \dfrac{c_s}{m_s} & 0 & \dfrac{c_s}{m_s} \\ 1 & -\dfrac{c_s}{m_s} & 0 & 0 \\ 0 & 0 & 1 & 0 \end{bmatrix}$$

C. RANDOM INPUT ROAD MODEL SIMULATION

Since vehicles running on different level of road will produce different vibration responses, the two-degree-of-freedom vehicle vibration model and random road model built above are used for software simulation based on MATLAB/Simulink.

According to the difference of road roughness coefficient, the road grade can be divided into 8 levels from A to H [25]. With the development of road construction in China, the domestic road levels are within the range of A, B, and C of the national standard. According to the actual road conditions, this paper selects four levels of roads A, B, C and D for research. The classification of different types of roads is shown in Table 1. The road roughness classification standard is shown in Table 2.

The parameters of vehicle come from Santana 3000, as shown in Table 3. The ride comfort simulation experiment is carried out on four types of roads, class A, B, C, and D. The driving speed is 20km/h, the simulation time is 60s, and the sampling frequency is 100Hz. The responses of vehicle on class B road are shown in Figure 7.
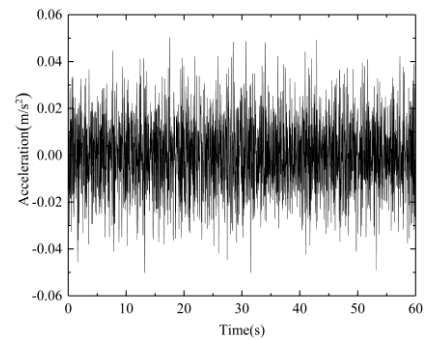
The root-mean-square values of vehicle vibration response under different grades of roads are shown in Table 4. It can

(a) Body acceleration

(b) Wheel acceleration

FIGURE 7. Vehicle responses on class B road.

be seen from it that as the road roughness level increases, the root-mean-square values of body acceleration and wheel acceleration increases, and the vibration amplitude increases.

IV. SIMULATION ANALYSIS
A. VEHICLE VIBRATION RESPONSE DATA SET

In the reverse identification of the road roughness level based on the vehicle responses, if features are extracted directly from the vehicle response signals, the resulting features will

TABLE 4. Vehicle Vibration Response Signals and Statistics.

Road roughness level	root-mean-square values	
	body acceleration	Wheel acceleration
Class A road	0.0074	0.0503
Class B road	0.0149	0.1007
Class C road	0.0333	0.2251
Class D road	0.0744	0.5033

TABLE 5. The Structure of The Vehicle Vibration Response Data Set.

Sample label	Road roughness level	Data segment
1	Class A road	119
2	Class B road	119
3	Class C road	119
4	Class D road	119
total		476

be too large and inconvenient to calculate. Therefore, in this paper the sliding window as 1s is used to adopted, which intercepts the vehicle response data as an equal length sequence of 100. In order to preserve the continuity of the signal, there is a 50% overlap between the two time periods. The constructed vehicle vibration response data set is randomly divided into two groups, 80% of which is selected as the training set and the rest is selected as the test set. The former is used for model training and the latter is used for model testing. The data segment of the vehicle vibration response is shown in Table 5.

B. EXPERIMENTS ON THE IDENTIFICATION OF ROAD ROUGHNESS LEVEL

The software environment for this experiment includes Python language and Keras deep learning framework. The hardware environment include Intel Core i5-4210U processor and graphics card AMD Radeon HD 8500M. Before the experiment, in order to improve the convergence speed and recognition accuracy, the vehicle vibration response data set is normalized, and the expression is shown in (14).

$$X_t = \frac{(x_t - x_{tmin})}{(x_{tmax} - x_{tmin})}(max - min) + min \tag{14}$$

where max and min express respectively the maximum and minimum values of scaling original data; x_{tmax} and x_{tmin} express respectively the maximum and minimum values of the vehicle response; x_t is the original data values; X_t is the normalized data values.

In addition, the Adam (adaptive moment estimation) optimizer is selected to optimize the model parameters. The Adam optimizer replaces the traditional stochastic gradient descent. It can update the network weight value based on the training data to realize the error back propagation, so that the loss function values are converged at the fastest speed.

(a) Loss function

(b) Accuracy
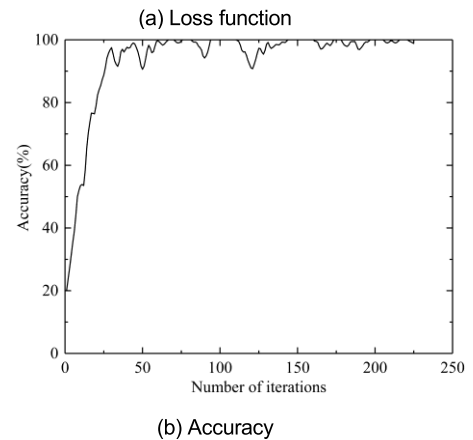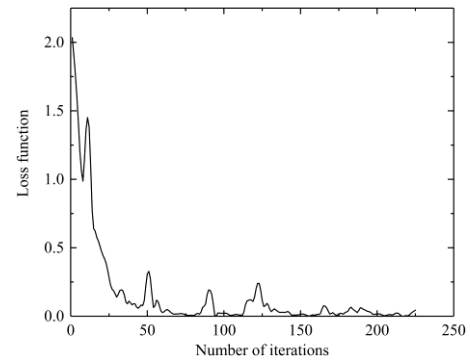
FIGURE 8. The training process of the model.

In order to further improve the efficiency of the algorithm and make the objective function converge smoothly, the mini-batch gradient descent method is adopted, and only a part of the mini-batch samples are selected for each training. The cross-entropy loss function is selected, and its expression is as follow:

$$loss = -\frac{1}{S}\sum_{S}\sum_{i=1}^{5} y'_i \ln(y_i) \tag{15}$$

where y'_i is the true probability of a certain sample sequence corresponding to the road roughness level category; y_i is the predicted probability of a certain sample sequence corresponding to the road roughness level category; S is the batch size, and the value is 32 during the experiment.

In the process of model training, the recognition accuracy and loss function are important indicators to evaluate the recognition effect of the model. The higher the recognition accuracy and the smaller the loss function, the better the model recognition effect and the higher the robustness. The training process of the model is shown in Figure 8.

It can be observed from Fig. 8(a) that the loss function has been showing a downward trend, and the decline speed is relatively fast. As the number of iterations increases, the loss function value approaches 0. Moreover, it can be observed from Fig. 8(b) that the accuracy rate of the model appears an upward trend as a whole, and the degree of shock is small. It only takes less training time to reach a higher accuracy, and
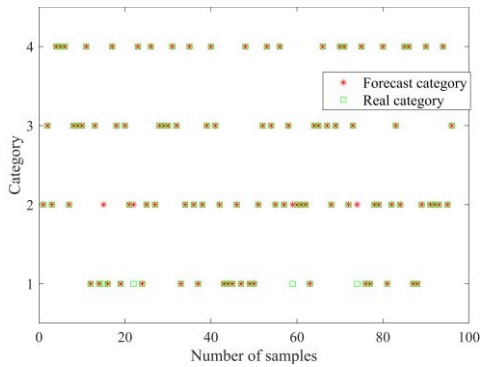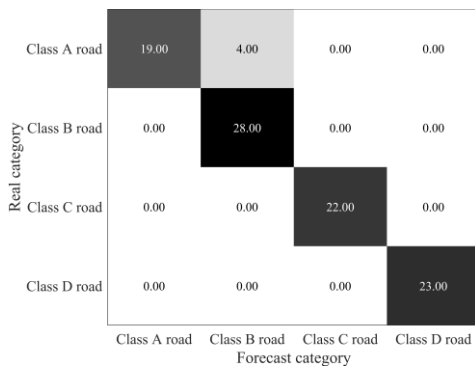
FIGURE 9. Test results.

FIGURE 10. Confusion matrix.

the accuracy approaches 100%,which shows that the model has good training effects and high accuracy.

The algorithm model is trained to determine the mapping relationship between the road level and the vehicle vibration responses, and then the test set is used to evaluate. Because the test set is completely separated from the model during the training process, the results of test can be used to evaluate the performance of the model. The result is shown in Fig. 9.

The confusion matrix of the test results is shown in Fig. 10. It can be seen from Fig. 10 that the prediction category of the road level by the identification model is very close to the real category distribution, and the recognition errors are mainly concentrated on the class A road and the class B road. That's probably because the vehicle vibration response characteristics corresponding to the two levels of roads are similar, which makes the model confuse them. As a result, the road roughness level of a small part of the data is incorrectly identified, which is consistent with the actual situation.

Table 6 shows the recognition accuracy of the road roughness level identification model, and the overall recognition rate is 95.83%. Experiments have proved that the model can achieve accurate classification for different road roughness levels.

C. THE IMPACT OF SPEED ON THE IDENTIFICATION RESULT

When the vehicle is moving, the speed is not constant. The above tests are accomplished at the speed of 20 km/h.

TABLE 6. Accuracy of Road Roughness Level Identification Model.

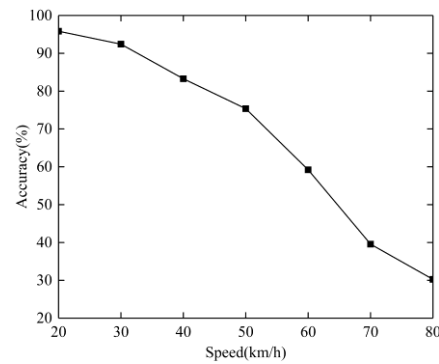| Road roughness level	Accuracy
Class A road	100%
Class B road	87.5%
Class C road	100%
Class D road	100%
Total recognition rate	95.83%

FIGURE 11. The overall recognition accuracy with different speed.

(a)Signal acquisition equipment   (b) Experimental vehicle

FIGURE 12. Experimental equipment.

Therefore, it is necessary to compare and analyze the recognition effect of the road roughness level identification model at other speeds. Another ride comfort simulation experiment is carried out at the speed of 20km/h, 30km/h, 40km/h, 50km/h, 60km/h, 70km/h, and 80 km/h. The simulation time is 10s, and the simulation frequency is 100 Hz. The data is sampled through 1s sliding window to form a standardized data, and the influence of speeds is analyzed. The overall recognition accuracy with different speed is as shown in Figure 11.

It can be seen from Figure 11 that the overall recognition accuracy of the model has been decreasing during the process of changing the speed from 20km/h to 80km/h. When the speed is within the range of 20km/h-40km/h, and the recognition accuracy is above 80%, which indicate that the road roughness level identification model has a good recognition effect at these speed. However, when the speed is higher than 40km/h, the recognition accuracy is reduced and the recognition effect becomes worse. That's because the road roughness level identification model is trained with vehicle vibration response data collected at a speed of 20km/h. When the speed changes greatly, the acquired characteristic signal
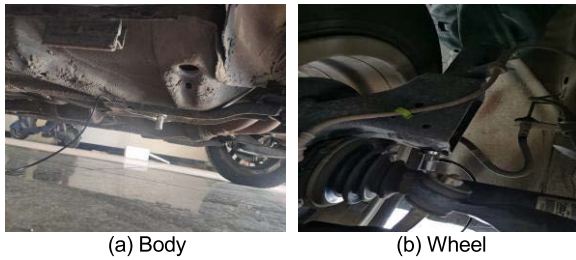
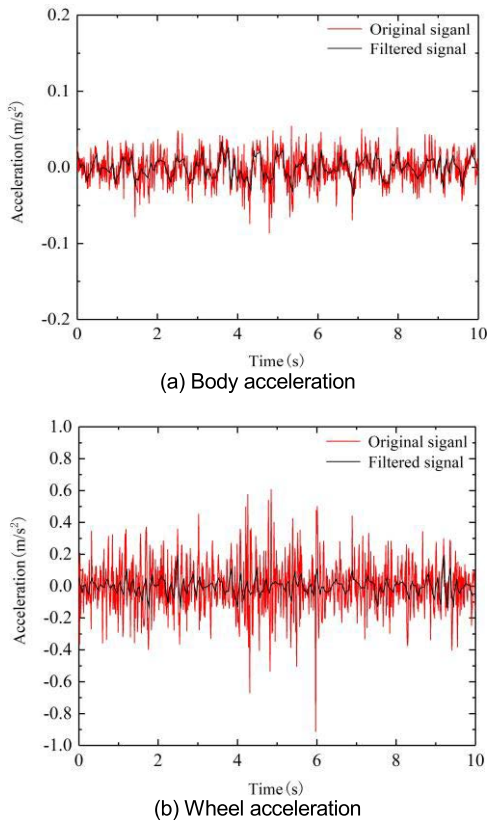**FIGURE 13.** Installation position of the acceleration sensor.

(a) Asphalt road   (b) Brick road

FIGURE 14. Experimental roads.

(a) Body acceleration

(b) Wheel acceleration

FIGURE 15. Vehicle responses on asphalt road.

(a) Body acceleration

(b) Wheel acceleration

FIGURE 16. Vehicle responses on brick road.

The experimental equipment used in this paper includes the vehicle, two acceleration sensors, NI USB-4431 data acquisition instrument, and computer, as shown in Figure 12.

The one of acceleration sensor is installed at the center of body mass of metal chassis, and another acceleration sensor is installed at the suspension arm of the right front wheel of the vehicle. The specific position is shown in Fig. 13. The selected roads include asphalt road and brick road, as shown in Fig. 14. In the process of experiment, vehicle is drove on the certain road at a constant speed of 20km/h for 10s every time, and the sampling frequency is 100Hz. The acceleration sensors are used to collect the electrical analog signals of vehicle vibration, and then they are converted into digital signals by data acquisition card, transmitted to the computer for storage.

B. PROCESSING OF EXPERIMENTAL DATA

In the experiment, there are unavoidable interference signals such as noise, so the experimental data need to be processed for noise reduction. In this paper, the wavelet method is used to process vehicle response signals [26], as shown in Figure 15 and 16. Its advantage is that the response signals can successfully reduce noise and retain the signal characteristics. Therefore, its performance is better than traditional noise reduction methods.

C. ANALYSIS OF RESULTS

The signals after noise reduction are used to form standardized data samples by the sliding window, and inputted into the

varies greatly. Therefore, in practical engineering applications, only when the vehicle should keep the speed in the range of 20km/h-40km/h, and the model has the best recognition effect on road roughness levels.

V. VEHICLE EXPERIMENTS

A. COLLECTION OF EXPERIMENTAL DATA

In order to verify the feasibility of the road roughness level identification model, vehicle experiments are carried out.
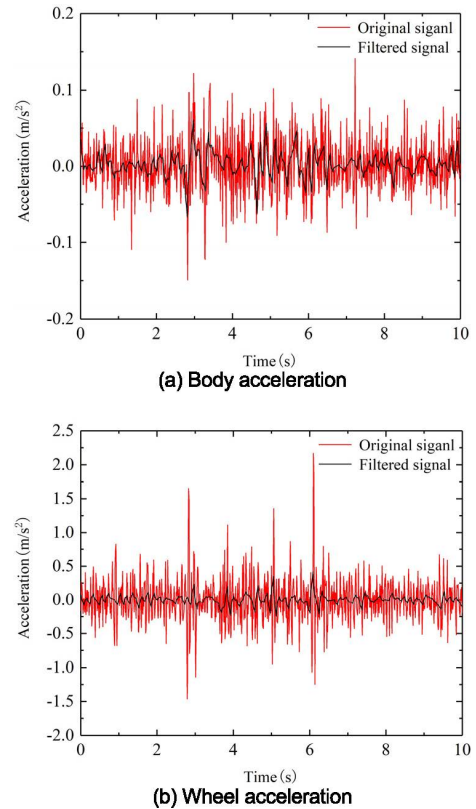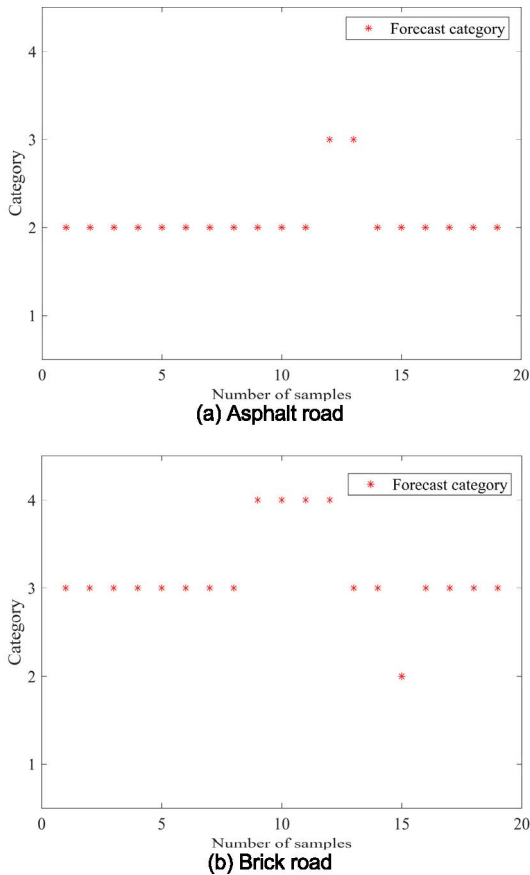
FIGURE 17. Recognition results of experimental road.

TABLE 7. Recognition accuracy of experimental roads.

Road type	Reference	Accuracy
Asphalt road	Class B road	89.47%
Brick road	Class C road	73.68%

VI. CONCLUSION

In this thesis, the reverse analysis of the vehicle vibration responses based on the BiGRU network is proposed to identify the level of road roughness. The recognition rate of the vehicle identification model with two-degree-of-freedom is as high as 95.83%. In order to verify the feasibility and practicability of the model, the ride comfort experiments are carried out on asphalt roads and brick roads, and the roughness levels of the experimental roads are successfully recognized.

In fact, the vehicle may be drove on more severe and complex roads, and the simulation data of the vehicle dynamics model cannot fully consistent with the vibration response of the vehicle on real roads. In the future, further researches should develop a large number of road experiments to build more integral data set, so that the road condition is more abundant, and the error of the recognition result is reduced.

road roughness level identification model after normalization to classify and identify the experimental road level, as shown in Figure 17.

The recognition accuracy of the experimental roads is shown in Table 7. The recognition accuracy of asphalt road is 89.47%, and the recognition accuracy of brick road is slightly worse than that of asphalt road, which is 73.68%. The reason is that the some sections of brick road are loose and not in good condition, which leads to poor ride comfort of the vehicle. Because of the increase of uncertain factors in the practical driving environment, the recognition accuracy of the model for the road roughness level under the vehicle experiment is lower than that of the simulation data, which is in line with the objective law. All of results show that the road roughness level identification model based on the BiGRU network can still effectively identify the level of road roughness in practical applications, and has good anti-interference, effectiveness.

REFERENCES

[1] *Standard Test Method for Measuring Pavement Roughness Using a Profilograph*, Standard ASTM E1274-18, 2008.

[2] V. Žuraulis, V. Surblys, and E. Šabanovič, "Technological measures of forefront road identification for vehicle comfort and safety improvement," *Transport*, vol. 34, no. 3, pp. 363–372, May 2019, doi: 10.3846/transport.2019.10372.

[3] M. A. Bekhyi and Y. Kobayashi, "Prediction of vibrations as a measure of terrain travers ability in outdoor structured and natural environments," in *Proc. 7th Pacific-Rim Sympo Image Video Technol.*, Auckland, New Zealand, 2015, pp. 282–294.

[4] Q. Liu, J. W. Sun, H. Zhang, X. Hu, and L. Gu, "Road identification and semi-active suspension control based on convolutional neural network," *Acta Armamentarii*, vol. 41, no. 8, pp. 1483–1493, Aug. 2020, doi: 10.3969/j.issn.1000-1093.2020.08.002.

[5] S. F. Wang, K. Y. Du, Y. Meng, and R. Wang, "Machine learning-based road terrain recognition for land vehicles," *Acta Armamentarii*, vol. 38, no. 8, pp. 1642–1648, Aug. 2017, doi: 10.3969/j.issn.1000-1093.2017.08.023.

[6] H. W. Xu, "Recognition of road moving target based on the time-frequency characteristics of millimeter wave radar," M.S. thesis, Xiamen Univ., Xiamen, China, 2019.

[7] H. M. Ngwangwa and P. S. Heyns, "Application of an ANN-based methodology for road surface condition identification on mining vehicles and roads," *J. Terramechanics*, vol. 53, pp. 59–74, Jun. 2014, doi: 10.1016/j.jterra.2014.03.006.

[8] H. M. Ngwangwa, "Road surface profile monitoring based on vehicle response and artificial neural network simulation," M.S. thesis, UP, Pretoria, South Africa, 2014.

[9] T. H. Nguyen, T. L. Nguyen, D. N. Sidorov, and A. I. Dreglea, "Machine learning algorithms application to road defects classification," *Intell. Decis. Technol.*, vol. 12, no. 1, pp. 59–66, Mar. 2018, doi: 10.3233/IDT-170323.

[10] C. Lin and Y. Shi, "Road roughness recognition based on NARX neural network," *J. Nanjing Univ. Sci. Technol.*, vol. 44, no. 3, pp. 296–302, Mar. 2020, doi: 10.14177/j.cnki.32-1397n.2020.44.03.006.

[11] J. Li, W. C. Guo, Q. Zhao, and S. F. Gu, "Study on road roughness identification based on four typical neural networks," *Automot. Eng.*, vol. 42, no. 1, pp. 100–107, Jan. 2020, doi: 10.19562/j.chinasae.qcgc.2020.01.015.

[12] J. Li, W. C. Guo, S. F. Gu, and Q. Zhao, "Road roughness identification based on NARX neural network," *Automot. Eng.*, vol. 41, no. 7, pp. 807–814, Jul. 2019, doi: 10.19562/j.chinasae.qcgc.2019.07.012.

[13] Y. Wang, G. Q. Liang, and Y. T. Wei, "Road identification algorithm of intelligent tire based on support vector machine," *Automot. Eng.*, vol. 42, no. 12, pp. 1671–1678, Dec. 2020, doi: 10.19562/j.chinasae.qcgc.2020.12.009.

[14] Z. Zhao, W. H. Chen, X. Wu, C. Y. Peter Chen, and J. M. Liu, "LSTM network: A deep learning approach for short-term traffic forecast," *IET Intell. Transp. Syst.*, vol. 11, no. 2, pp. 68–75, Feb. 2017, doi: 10.1049/iet-its.2016.0208.

[15] S. T. Ding and S. R. Qu, "Traffic object detection based on deep learning with region of interest selection," *China J. Highway Transp.*, vol. 31, no. 9, pp. 167–174, Sep. 2018.

[16] G. V. Konoplich, E. O. Putin, and A. A. Filchenkov, "Application of deep learning to the problem of vehicle detection in UAV images," in *Proc. 15th IEEE Int. Conf. Soft Comput. Meas. (SCM)*, May 2016, pp. 4–6.

[17] Y. F. Cai, K. S. Tai, H. Wang, W. C. Li, and L. Chen, "Research on behavior recognition algorithm of surrounding vehicles for driverless car," *Automot. Eng.*, vol. 42, no. 11, pp. 1464–1472, Oct. 2020, doi: 10.19562/j.chinasae.qcgc.2020.11.003.

[18] L. Cheng, X. Zhang, and J. Shen, "Road surface condition classification using deep learning," *J. Vis. Commun. Image Represent.*, vol. 64, Oct. 2019, Art. no. 102638, doi: 10.1016/j.jvcir.2019.102638.

[19] G. Q. Liang, T. Zhao, Y. Wang, and Y. T. Wei, "Road unevenness identification based on LSTM network," *Automot. Eng.*, vol. 43, no. 4, pp. 509–517, Apr. 2021, doi: 10.19562/j.chinasae.qcgc.2021.04.008.

[20] S. Hochreiter and J. Schmidhuber, "Long short-term memory," *Neural Comput.*, vol. 9, no. 8, pp. 1735–1780, Nov. 1997, doi: 10.1162/neco.1997.9.8.1735.

[21] K. Cho, B. van Merriënboer, C. Gulcehre, D. Bahdanau, F. Bougares, H. Schwenk, and Y. Bengio, "Learning phrase representations using RNN encoder-decoder for statistical machine translation," *Comput. Sci.*, pp. 1724–1734, Oct. 2014, doi: 10.3115/v1/D14-1179.

[22] W. W. Li, Q. Shi, K. Wang, and X. Cheng, "Runoff prediction based on variational mode decomposition and deep gated network," *J. Hydroelectric Eng.*, vol. 39, no. 3, pp. 34–44, Mar. 2020, doi: 10.11660/slfdxb.20200304.

[23] J. H. Zhao, Z. R. Wang, and Z. L. Guan, "The representation method of road roughness data," in *Analysis and Application of Road Roughness Measurement*. 2000, pp. 108–131.

[24] F. Yu and Y. Lin, "Pavement model and comfort standards," in *Automobile System Dynamics*, 2nd ed. 2017, pp. 153–171.

[25] Z. S. Yu, "Ride comfort," in *Theory of Automobile*. 2000, pp. 203–210.

[26] Y. C. Qin, M. M. Dong, F. Zhao, and L. Gu, "Vehicle semi-active suspension control based on road surface recognition," *J. Northeastern Univ. Natural Sci.*, vol. 37, no. 8, pp. 1138–1143, Aug. 2016, doi: 10.12068/j.issn.1005-3026.2016.08.016.

SHUANG CHEN received the Ph.D. degree in vehicle engineering from Jilin University, Changchun, China, in 2012.

She is currently a Professor at the College of Automobile and Traffic Engineering, Liaoning University of Technology, Jinzhou, China. She has authored or coauthored more than 40 journals and conference papers. She is in charge of numerous projects funded by national government and institutional organizations. Her current research interests include vehicle system dynamics and control, vehicle safety and intelligent control technology, and key technologies of intelligent networked new energy vehicles.

JUNJUN XUE is currently pursuing the degree with the Liaoning University of Technology.

• • •